www.czasopisma.pan.pl PAN POLSKA AKADEMIA NAUK www.journals.pan.pl

jet INTL JOURNAL OF ELECTRONICS AND TELECOMMUNICATIONS, 2021, VOL. 67, NO. 4, PP. 615-621
Manuscript received February 26, 2021; revised November, 2021 DOI:10.24425/ijet.2021.137854

Micromechanically Tunable Dielectric Rod Resonator

Kostiantyn Savin, Irina Golubeva, Victor Kazmirenko,
Yuriy Prokopenko, and Guy A. E. Vandenbosch

***Abstract*—A resonant frequency control method for dielectric rod resonators is discussed. A dielectric rod of cylindrical shape is placed inside a metal cavity. The bottom face of the dielectric rod is fixed at the metal base plate. Resonant frequency tuning is achieved by lifting the top metal plate above the dielectric rod upper face. The paper presents simulations using the mode matching technique and experimental study of this tunable resonator. Resonant frequency of the basic mode can be tuned by more than an octave with displacements of only tens of micrometres, which is in range of piezoactuators, MEMS, etc. A distinct feature of the proposed tuning technique is that the quality factor of the system does not degrade throughout the tuning range.**

***Keywords*—dielectric resonator, resonant frequency, electromechanical tuning, quality factor, mode matching technique**

I. Introduction

DIELECTRIC resonators (DRs) are widely used in modern radiofrequency equipment because of their small size and high quality (Q) factor [1]—[4]. The tunable DR with high-Q performance within the whole tuning range is highly demanded for various components of communication devices, like filters, phase shifters, oscillators, etc.

One of the most common ways to obtain tunability is adding varactors to the electric circuit of a resonant element [5]. This approach leads to additional loss of electromagnetic energy. Thus, it is not appropriate for high-Q applications. On the other hand, using a mechanical tuning allows maintaining the Q-factor of the initial resonant element [6], [7]. As all electric ways of control are desired in practical applications, there are attempts to combine mechanical and electrical control [8]. Fast tuning can be achieved by using piezoelectric, electrostrictive actuators. However, their fast operation speed comes at the expense of a rather small displacement. Thus, the design should show a high sensitivity of the resonant frequency to the mechanical displacement of the device's parts in order to benefit from the actuator's operation speed.

The dielectric rod resonator short circuited at both ends is well studied and widely used thanks to its small dimensions and superior quality factor [9]. The research presented here adds tuning capability to the considered resonator.

A dielectric rod with relative permittivity ε of cylindrical shape with radius R and height h is fixed at the bottom plate of a surrounding metal cavity of radius R_s. The upper metal plate of the cavity can move above the dielectric rod top surface, opening an air gap of height d, Fig. 1.

A variation of the air gap height d causes an electromagnetic field redistribution, which results in a resonant frequency shift. Therefore, tuning is achieved by moving the perturber, i.e. the upper metal plate above the dielectric rod face.

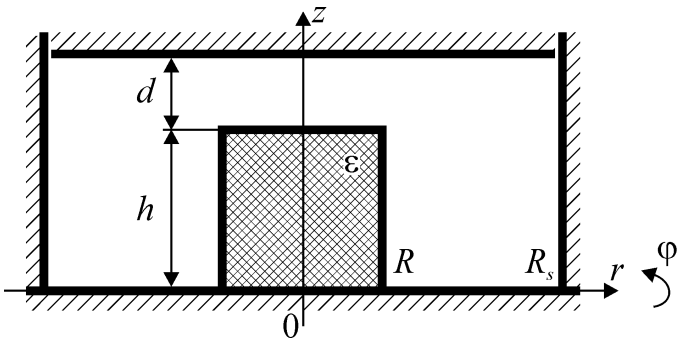

Fig. 1. Tunable schielded cylindrical dielectric resonator.

Certain resonant modes are very sensitive to the air gap height, i.e. the metal plate displacement. The following report demonstrates the wide range resonant frequency tuning with displacement of a few percent of the rod height. In X-band a tuning over an octave could be achieved with displacements of just tens of micrometres. Such a displacement is in the range of available piezo motors, MEMS etc. Thus, an electromechanical type of tuning can be implemented.

This paper reports on the innovating tunable resonator, and presents a study of the resonant frequency tunability and quality factor of the multiple modes with respect to the design parameters, such as, dielectric rod and cavity radii, dielectric rod permittivity and height, dielectric and metal losses. A comparison of the proposed tunable resonator with literature is presented in Table I. This shows that our proposal provides a high-end solution, usable in case when performance is crucial and cost is less of an issue.

TABLE I
COMPARISON OF STUDIED RESONATOR WITH LITERATURE

Ref	Operational frequency [GHz]	Unloaded Q-factor	Tuning range	Robustness	Cost
[9]	~ 5	~ 25–50	~ 15%	high	low
[11]	~ 3	~ 50	~ 20%	high	low
[12]	~ 4	~ 120	~ 1.2%	high	medium
[13]	~ 3	~ 10	~ 50%	high	low
[14]	~ 15	~ 50–200	~ 20%	low	high
[15]	~11.5	~ 300	~ 4.3%	high	low
This work	~ 2.4	~ 2000	~ 100%	medium	high

K. Savin, I. Golubeva, V. Kazmirenko, and Yu. Prokopenko are with the Department of Electronic Engineering, Igor Sikorsky Kyiv Polytechnic Institute, Kyiv, Ukraine (e-mail: v.kazmirenko@ieee.org).

G. A. E. Vandenbosch is with ESAT-TELEMIC Group, KU Leuven, Leuven 3000, Belgium (e-mail: guy.vandenbosch@esat.kuleuven.be).

II. Research Technique

A. Simulation

The resonator topology under consideration was simulated by using the mode matching technique (MMT), similarly to [16]. This technique was adapted to cope with the very small air gap height. These adaptions are briefly described, without going into full detail. Unlike in [16], the problem was formulated in terms of a reduced set of Fredholm's integral equations of the first kind with respect to auxiliary functions, which are proportional to the z-component of the electric and magnetic field [17]. Auxiliary functions were used to describe the electromagnetic field distribution. The Galerkin method was applied to solve this set of integral equations. The auxiliary functions were expanded with respect to a specific basis. This transforms the problem into a homogenous system of linear equations in the coefficients of the series expansion. The requirement of finding a nontrivial solution of this system results in a nonlinear eigen value problem. This eigen value defines the resonant frequency, and the eigen vector defines the respective electromagnetic field configuration, i.e. the resonant mode [18].

According to [9], at zero air gap $d = 0$ resonant modes are classified as HE_{nml}, EH_{nml}, TM_{0ml}, TM_{nm0} and TE_{0ml}. In the presence of the air gap, $d \neq 0$, the last index in the mode classification is not an integer any more. However, we keep the Kobayashi notation [9] as these modes have a similar field configuration in the cross section.

The Galerkin method was implemented using two sets of basis and test functions. One set employs axial eigen functions of domains, representing volumes inside and outside of the rod, i.e. for $r < R$ and $r > R$, respectively. Solutions obtained in this way coincide well with those of [16]. Another set accounts for the singularity of the electromagnetic field distribution near the dielectric edge $E \sim r^{\nu-1/2}$ [19], where r is the distance to the edge, and

$$\nu = \frac{1}{\pi}\arccos\left(\frac{\varepsilon^2+6\varepsilon+1}{2\varepsilon^2+4\varepsilon+2}\right)-\frac{1}{2}.$$

To arrange basis and test functions with similar singularity the ultraspherical (Gegenbauer) polynomials $C_{2l}^{\nu}(\tilde{z}), C_{2l+1}^{\nu}(\tilde{z})$ were used. These polynomials are orthogonal with weights $\left(1-\tilde{z}^2\right)^{\nu-1/2}$ and complete on the interval [0, 1].

Because these basis and test functions are very close to the actual distribution of the electromagnetic field, the numerical method converges extremely fast, with a very small number of functions, see Fig. 2.

As will be demonstrated later, a better tunability is achieved as the R/h ratio increases. Still, for most practical applications, even in case of higher permittivities or higher order modes, a sufficient accuracy for the *TM*- and *HE*-modes is reached with less than 10 basis and test functions.

As also seen in Fig. 2, the relative error of the technique is much smaller in case of *TE*- and *EH*-modes. The convergence of the simulation results for these modes is fast due to the continuity of the axial component of the electric field in the axial direction, which in turn results in a poor resonant frequency tunability. In general, the simulation of highly tunable modes requires a larger set of basis and test functions to achieve a target accuracy.

The presented simulation technique gives results very close to other methods, such as the finite elements method, and the finite integration technique [17].

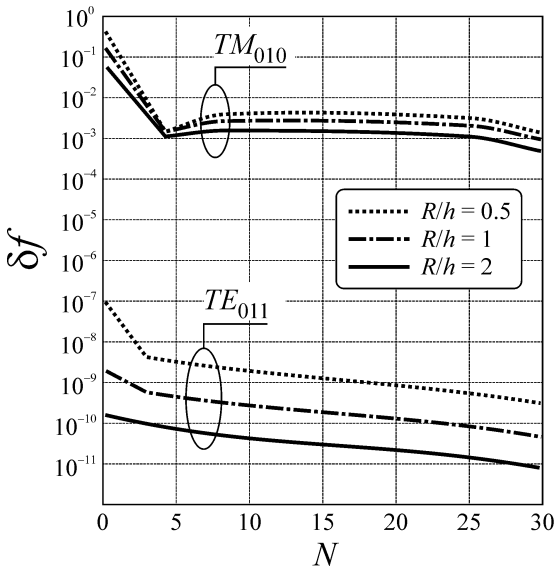

Fig. 2. Relative computational error of resonant frequency δf for TM_{010} and TE_{011} modes versus the number N of basis and test functions. $d/h = 0.02$, $R_s/R = 2$, $\varepsilon = 80$.

B. Experimental study

The experimental prototype is shown in Fig. 3. Its basic component is a brass enclosure of inner radius 12 mm (Fig. 3, top left) which provides the bottom plate and the metal shield. There are two coaxial ports in the side wall of the enclosure which provide resonator excitation using coupling loops. Two cylindrical dielectric rods were used in the experiment (Fig. 3, bottom left). The first rod is of radius 7 mm, height 4.5 mm and permittivity 37.7. The second rod is of radius 5.5 mm, height 5 mm and permittivity 79.

A brass piston of radius 11.75 mm was used as a movable upper plate. This piston is attached to a Digimatic micrometre head, series 350 (Fig. 3, right). A N5247A PNA-X Microwave Network Analyzer was used to measure the two-port *S*-parameters of the device.

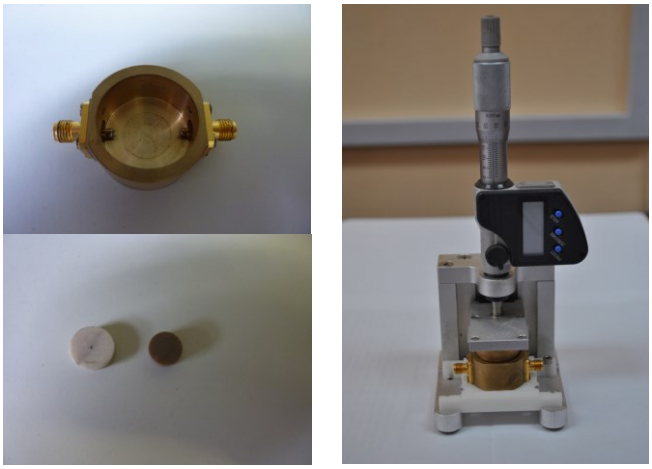

Fig. 3. Experimental setup. Top left: metal enclosure, bottom left: dielectric resonators used in experiment, right: metal cylinder attached to the micrometer head.

Note that the upscaled dimensions of both resonator and cavity were used intentionally in the experiment in order to ensure the accuracy of the displacement setting with the micrometre screw. A practical design using a real electromechanical way of controlling can be implemented at a much smaller scale, where the displacement can be kept within a range of tens of micrometres. Other design considerations will be presented in the next section.

The measured frequency dependencies of the *S*-parameters near the resonance were approximated using circuit theory models [20]:

$$S_{11}(f_o) = \frac{1+j\xi}{1+j\xi+K};$$

$$S_{21}(f_o) = \frac{K}{1+j\xi+K},$$

where $\xi = Q_0\left(\frac{f}{f_o} - \frac{f_o}{f}\right)$; f_o is the operating frequency; f is the resonant frequency; Q_0 is the unloaded quality factor; K is the coupling coefficient at the resonant frequency. The resonant frequency f, unloaded quality factor Q_0, and coupling coefficient K were derived as solutions of the minimization problem:

$$\min_{f,Q_0,K} \sum_{i=1}^{N} \left[\left(S_{11}(f_{o_i}) - S_{11_i}^{\exp} \right)^2 + \left(S_{21}(f_{o_i}) - S_{21_i}^{\exp} \right)^2 \right],$$

where $S_{11_i}^{\exp}$, $S_{21_i}^{\exp}$ are the values of the scattering parameters, measured at the operating frequency f_{o_i}.

The theoretical and experimental results for the resonant frequencies of the TM_{010} and the TE_{011} mode are compared in Fig. 4. Measured results are in good agreement with simulated results. For the TM_{010} mode, the tuning range of sample 1 reaches 0.9 GHz (38%) at a displacement of the moving metal plate of about 300 μm, while for sample 2 a tuning range of 0.95 GHz (43%) is obtained by moving the metal piston about 350 μm. Similarly, for the TE_{011} mode a resonant frequency shift of 0.3 GHz (7%) is obtained by moving the metal plate over 800 μm.

III. Discussion

A number of distinct modes can be excited in the structure under consideration, such as HE_{nml}, EH_{nml}, TM_{0ml}, TM_{nm0} and TE_{0ml}. From a tunability point of view, these modes exhibit a different sensitivity to the variation of the air gap. This depends on the configuration of the electric field along the direction of the perturber movement. In general, modes having a dominant component of the electric field normal to the resonator face adjacent to the moving plate, i.e. in 0*z* direction, demonstrate a larger frequency shift for the same displacement of the metal plate. In such a configuration the electric field distribution experiences a strong discontinuity at the air-dielectric boundary, which also strongly depends on the air gap height. Thus, a small displacement of the plate above the resonator face causes a significant redistribution of the electromagnetic field, which is observed as a resonant frequency shift. Among all mentioned modes, this requirement is best satisfied for the TM_{mn0} family.

The resonator tuning under the form of a resonant frequency shift is caused by the redistribution of the electromagnetic field along the axis of the plate movement, i.e. in 0*z* direction. As

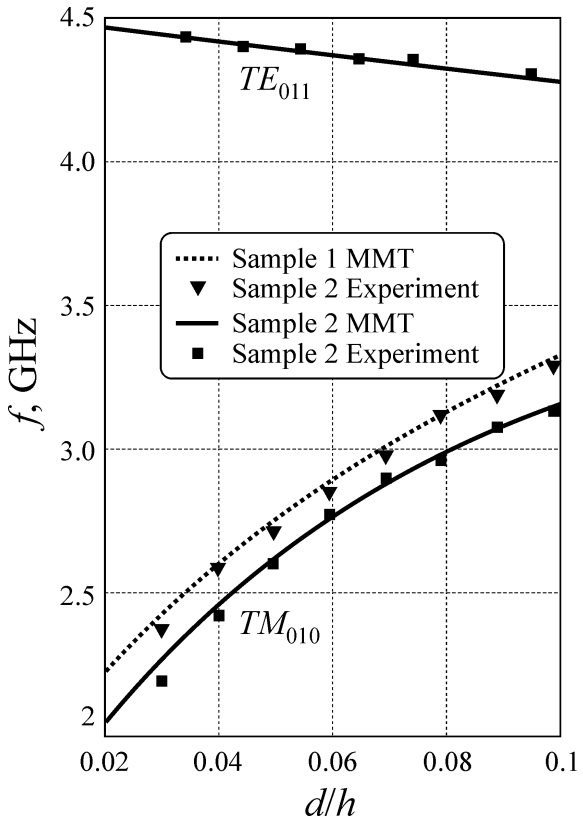

Fig. 4. Resonant frequency of TM_{010} and TE_{011} modes versus normalized air gap thickness calculated using MMT and measured experimentally in case of R_S=12 mm and: 1) R=7 mm, h=4.5 mm, ε=37.7, 2) R=5.5 mm, h=5 mm, ε=79.

seen in Fig. 5, the electric field of the TM_{010} mode outside the dielectric rod experiences a significant reconfiguration if the air gap varies. TM_{mn0} modes with larger m, n indices have significant components in the other directions, which do not participate in the field redistribution. Therefore, these modes exhibit a smaller tunability compared to the TM_{010} mode.

As seen in Fig. 6, the resonant frequency of the TM_{010} mode is very sensitive to variations of the air gap height d. An alteration of d in the order of only a few percents of h leads to a resonant frequency shift in the order of tens of percents. Such sensitivity gives an opportunity to apply piezoelectric actuators or MEMS for resonant frequency tuning.

At the same time, the sensitivity and tuning range of the nearest TM_{110} mode is smaller compared to TM_{010}, see Fig. 6. Nevertheless, this mode is of great practical interest, as it is excited in the resonator placed into a rectangular waveguide without any additional coupling elements [21]. However, for the TM_{110} mode over half the maximum possible tuning is achieved with a displacement under 5% of the rod height. Both sensitivity and tuning range versus air gap height increase with larger values of the dielectric rod permittivity, see Fig. 6.

The tuning range and the resonant frequency sensitivity of the TM_{010} mode both rise as the R/h ratio increases, see Fig. 7. Considering the limit $R/h \to \infty$ one may get extreme tuning characteristics. In this case, the problem reduces to a one-dimensional dielectric discontinuity situated between infinitely wide conductors, and the wavelength tuning can be described using the effective permittivity. The effective relative permittivity ε_{ef} is defined as the permittivity of a uniform

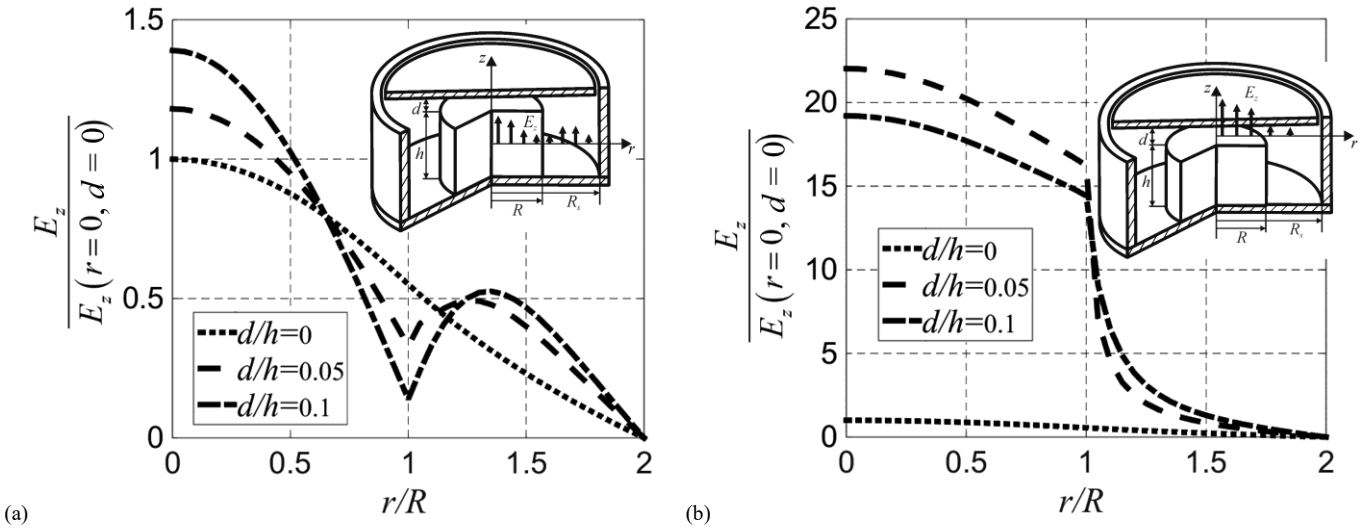

Fig. 5. TM_{010} mode normalized z-components of electric field in radial direction: (a) at $z = h/2$; (b) at $z = h+d/2$. $R_S/R = 2$, $\varepsilon = 80$, $R/h = 2$.

structure with the same wavelength as the non-uniform structure under consideration. The problem has an analytical solution [22]:

$$\varepsilon_{ef} = \varepsilon \frac{h+d}{h+\varepsilon d}. \quad (1)$$

A maximum possible frequency tuning can be estimated by using the technique presented in [9] for a uniform shielded resonator, but substituting the permittivity defined in (1). As illustrated in Fig. 8, the maximum possible tuning limit is achieved for $R/h \to \infty$. The value of that limit depends on the dielectric rod permittivity, see Fig. 6.

The resonant frequencies of the TM_{0ml} and HE_{nml} modes can be tuned by movement of the metal plate as well. However, as is the case for the sensitivity, the tuning range is smaller compared to the TM_{010} or TM_{110} modes. In contrast, the resonant frequencies of the TE_{0ml} and EH_{nml} modes demonstrate a very small variation with the air gap height, see Fig. 4. Moreover, their variation trend is opposite to those of the TM_{mn0}, TM_{0ml}, and HE_{nml} modes. These modes demonstrate a poor tunability, as they have no dominant z-component of the electric field at the rod face.

It is important to point out that the resonant frequency tuning range can be limited by the presence of closely spaced neighbouring modes, which could result in unsolicited transmission or rejection bands. However, as the air gap changes the resonant frequency shift direction depends on particular mode peculiarities. For instance, as the air gap grows the resonant frequency of the *TM* or *HE*-mode increases, but it decreases for the *TE* or *EH*-mode. This means that there can be values of the air gap for which resonant frequencies of different modes degenerate and change their position in the spectrum as the gap continues to grow. This case is illustrated in Fig. 9. Besides the just considered situation, adjacent *TM* modes, as well as *HE* modes can swap their spectral positions if the air gap grows. Thus, the device should be designed and constructed in such a way that neighbouring modes do not degenerate throughout the working displacement range.

As an example of a design rule one may require that in the absence of the air gap the wavenumbers of the neighbouring

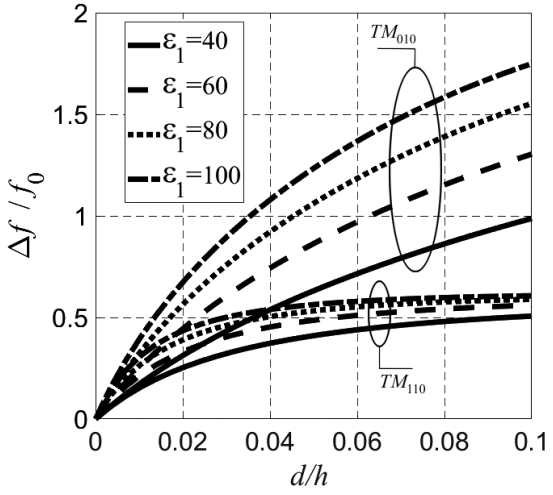

Fig. 6. Normalized TM_{010}, TM_{110} modes resonant frequency tuning versus gap to rod height ratio with $R_S/R = 2$, $R/h = 2$.

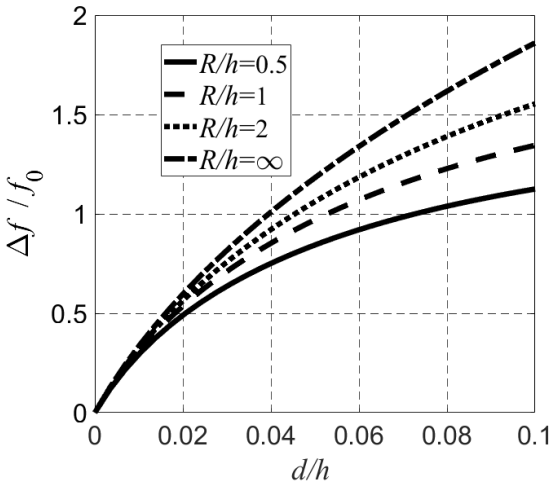

Fig. 7. Normalized TM_{010} mode resonant frequency tuning versus gap to cylinder height ratio. $R_S/R = 2$, $\varepsilon = 80$.

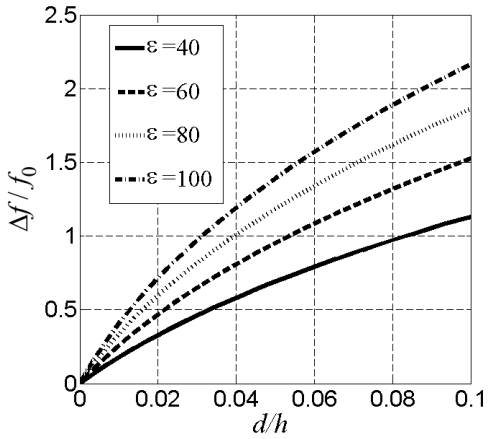

Fig. 8. Maximum possible normalized TM_{010} mode resonant frequency tuning versus air gap to cylinder height ratio; $R_S/R = 2$, $R/h \to \infty$.

modes should exceed the wavenumber of the operating mode with a margin large enough to avoid their degeneration during d/h tuning. The dependencies of the lowest modes' initial wavenumbers depicted in Fig. 10, Fig. 11 give an idea about a proper design parameter selection. For instance, with $R/h < 0.5$ and $R_S/R < 2$ the EH_{111} mode degenerates with TM_{110}, see Fig. 10, Fig. 11. To avoid such limitation on the TM_{110}-mode tuning range one has to:

- reduce the cylinder height in order to rise the *EH*, *TE* modes' wavenumbers;
- increase the cylinder to shield distance (R_S/R ratio) to reduce the *TM*-modes' wavenumbers.

This described design freedom is possible, because the resonant frequencies of the *EH*, *TE* modes weakly depend on the dielectric permittivity, while the resonant frequencies of the TM_{mn0} modes practically do not depend on the R/h ratio.

IV. QUALITY FACTOR

The unloaded quality factor Q_0 of the resonator, defined by the dielectric loss and the metal loss, can be expressed as

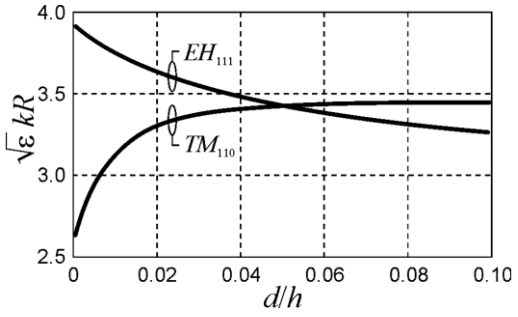

Fig. 9. Degeneration of EH_{111} mode with TM_{110} when gap exceeds $d/h = 0.05$; $R/h = 1$, $R_S/R = 2$.

$$Q_0^{-1} = Q_d^{-1} + Q_m^{-1}, \tag{2}$$

where Q_d is the unloaded Q factor caused by the dielectric loss, and Q_m is the unloaded Q factor caused by the metal loss. The metal loss is concentrated in the parallel plates rather than in the shield. Q_d and Q_m were obtained with the mode matching technique used to calculate the electromagnetic field distribution [23].

As seen in Fig. 12, the Q factor caused by the dielectric loss increases as the air gap height increases. The fundamental reason of this behavior is a redistribution of the electromagnetic energy from the dielectric rod to the air gap. Since air has very low loss this decreases the dielectric loss.

It also follows that an increase of the dielectric rod height results in a decrease of the Q factor caused by the dielectric loss. The reason is the internal reflection effect inside the dielectric cylinder. Thus, a change of the geometrical or electrical parameters which results in a wider tuning range also leads to a higher Q factor caused by the dielectric loss. Considering the limit $R/h \to \infty$, one may note an extreme quality factor, which is not reachable in any practical design.

The dependency of the normalized quality factor of the TM_{010} mode caused by the metal loss versus normalized air gap

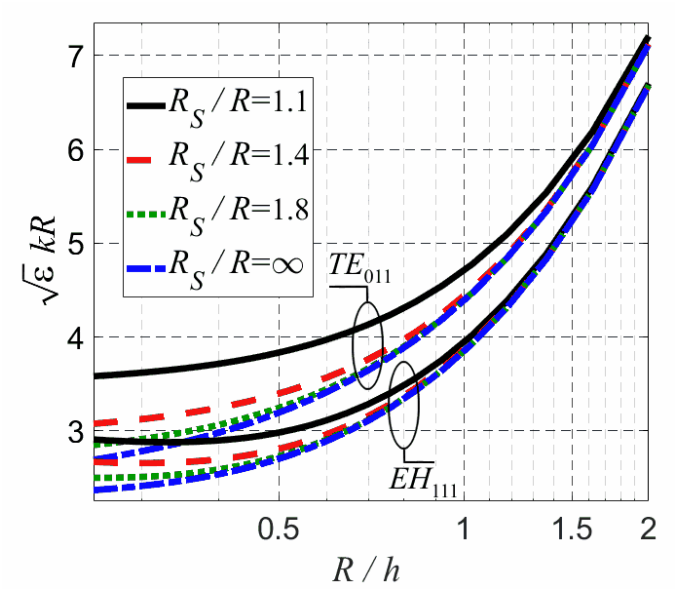

Fig. 10. Normalized resonant wavenumber of EH_{111} and TE_{011} modes versus dielectric cylinder height to radius ratio in the absence of air gap $d = 0$, ε=80.

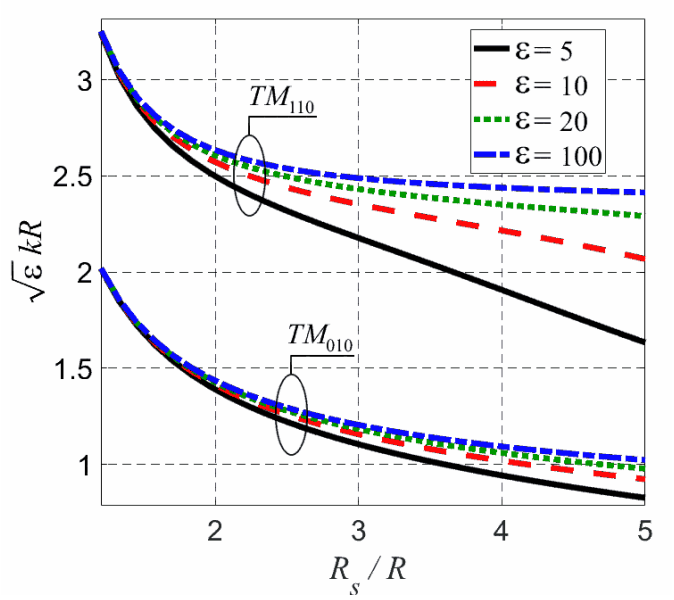

Fig. 11. Normalized resonant wavenumber of TM_{010} and TM_{110} modes versus shield to dielectric cylinder radius ratio in the absence of air gap $d = 0$.

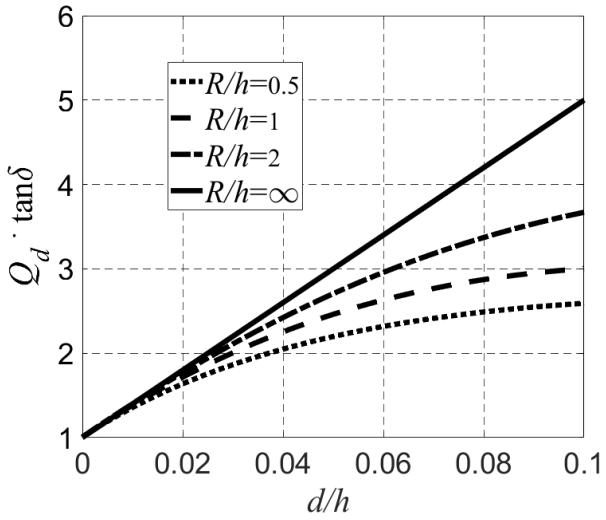

Fig. 12. Normalized Q factor of the TM_{010} mode caused by dielectric loss versus normalized air gap dimension for tunable shielded cylindrical metal-dielectric resonator with following parameters: R_S = 2R, ε = 40.

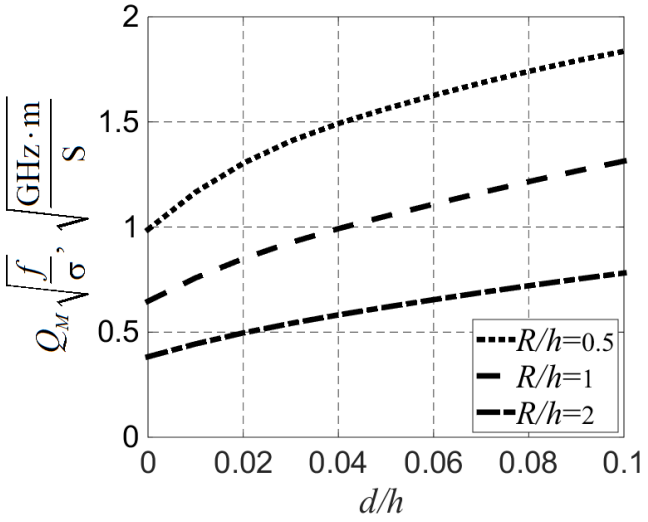

Fig. 13. Normalized Q factor of the TM_{010} mode caused by metal loss versus normalized air gap dimension for tunable shielded cylindrical metal-dielectric resonator with following parameters: R_S = 1.5R, ε = 30.

height for various values of the normalized height is presented in Fig. 13.

It is seen that the Q factor caused by the metal loss increases as the air gap height increases. The reason is an increase of the overall height of the resonator. Thus, the volume of the resonator increases while the area corresponding to the parallel metal plates remains constant. The result is a redistribution of the electromagnetic energy from the metal plates to the volume of the cavity.

It is also seen that an increase of the dielectric cylinder height results in an increase of the Q factor caused by the metal loss. Thus, a change of geometrical or electrical parameters which results in a wider tuning range leads to a lower Q factor caused by the metal loss. So, a trade-off between wider tuning range and Q factor caused by dielectric loss on the one hand and Q factor caused by metal loss on the other hand is necessary.

V. Conclusion

It has been shown that in a tunable schielded cylindrical dielectric resonator only modes with a predominant component of the electric field in the direction normal to the moving metal perturber exhibit superior tuning capabilities. The TM_{010} mode demonstrates a maximum tuning range and sensitivity to the control factor: in an X-band device, the resonant frequency shifts more than an octave with a displacement of only tens of micrometres. In practice, such a small displacement requires the use of micromechanical drivers such as piezoelectric components, MEMS, etc.

For waveguide type applications the TM_{110} mode is of particular interest. Despite of the somewhat smaller tuning range and sensitivity compared to TM_{010}, this mode is reliably excited in a rectangular waveguide without extra coupling elements.

It has been shown that the tuning range of an operating mode is limited by the vicinity of neighbouring modes. This limitation can be relieved by reducing the height of the dielectric rod, or by increasing the shield radius. The unloaded Q factors caused by metal loss and dielectric loss both grow as gap height increases. Therefore, the presented tunable resonator is able to maintain its high level of Q factor when the resonant frequency is tuned.

References

[1] J. X. Xu, X. Y. Zhang and Q. Xue, "Dual-channel filter based on dielectric resonator for 5G massive MIMO system," 2018 IEEE MTT-S International Wireless Symposium (IWS), Chengdu, 2018, pp. 1-3. https://doi.org/10.1109/IEEE-IWS.2018.8400849

[2] A. Panariello, M. Yu and C. Ernst, "Ku-Band High Power Dielectric Resonator Filters," in IEEE Transactions on Microwave Theory and Techniques, vol. 61, no. 1, pp. 382-392, Jan. 2013. https://doi.org/10.1109/TMTT.2012.2229292

[3] A. Rashidian and L. Shafai, "Low-Profile Dielectric Resonator Antennas for Millimeter-Wave Applications", in 15th Int. Symp. Antenna Technol. Appl. Electromagn., 2012. https://doi.org/10.1109/ANTEM.2012.6262406

[4] C. Orlob and C. Neumaier, "Tunable quad-mode dielectric resonator filter," 2017 47th European Microwave Conference (EuMC), Nuremberg, 2017, pp. 915-918. https://doi.org/10.23919/EuMC.2017.8230994

[5] F. Lin and M. Rais-Zadeh, "Continuously Tunable 0.55–1.9-GHz Bandpass Filter With a Constant Bandwidth Using Switchable Varactor-Tuned Resonators," IEEE Trans. Microw. Theory Tech., vol. 65, no. 3, pp. 792–803, March 2017. https://doi.org/10.1109/TMTT.2016.2633270

[6] J. Uher and W. J. R. Hoefer, "Tunable microwave and millimeter-wave band-pass filters," in *IEEE Transactions on Microwave Theory and Techniques*, vol. 39, no. 4, pp. 643-653, Apr 1991. https://doi.org/10.1109/22.76427

[7] Tao Shen, K. A. Zaki and Chi Wang, "Tunable dielectric resonators with dielectric tuning disks," in *IEEE Transactions on Microwave Theory and Techniques*, vol. 48, no. 12, pp. 2439-2445, Dec 2000. https://doi.org/10.1109/22.898995

[8] F. Huang, S. Fouladi, and R. Mansour, "High-Q tunable dielectric resonator filters using MEMS technology", IEEE Trans. Microw. Theory Tech., vol. 59, no. 12, pp. 3401–3409, Dec. 2011. https://doi.org/10.1109/TMTT.2011.2171984

[9] Y. Kobayashi, S. Tanaka, "Resonant modes of a dielectric rod resonator short-circuited at both ends by parallel conducting plates," IEEE Trans. Microw. Theory Tech., vol. 28, no 10, pp.1077-1085, Oct. 1980. https://doi.org/10.1109/TMTT.1980.1130228

[10] M. Esmaeili, J. Bornemann, "Novel Tunable Bandstop Resonators in SIW Technology and Their Application to a Dual-Bandstop Filter with One Tunable Stopband," IEEE Microw. Wirel. Compon. Lett., vol. 27, no 1, pp. 40–42, Jan. 2017. https://doi.org/10.1109/LMWC.2016.2630007

[11] B. Potelon, C. Quendo, E. Rius, J.-F. Favennec, "Tunable Bandstop Resonator based on Dual Behavior Resonator Principle," Proceedings of

2017 IEEE Africon, Cape Town, 2017, pp. 559–562. https://doi.org/10.1109/AFRCON.2017.8095542

[12] J. Berge, A. Vorobiev, W., and S. Gevorgian, "Tunable Solidly Mounted Thin Film Bulk Acoustic Resonators Based on BaxSr1-xTiO3 Films," IEEE Microw. Wirel. Compon. Lett., vol. 17, no 9, pp. 655–657, Sep. 2007. https://doi.org/10.1109/LMWC.2007.903445

[13] R. Allanic, D. Le Berre, Y. Quéré, C. Quendo, D. Chouteau, V. Grimal, D. Valente, and J. Billoué, "Continuously Tunable Resonator Using a Novel Triangular Doped Area on a Silicon Substrate," IEEE Microw. Wirel. Compon. Lett., vol. 28, no 12, pp. 1095–1097, Dec. 2018. https://doi.org/10.1109/LMWC.2018.2877661

[14] R.R. Benoit, N.S. Barker, "Superconducting Tunable Microstrip Gap Resonators Using Low Stress RF MEMS Fabrication Process" IEEE J. Electron Devices Soc., vol. 5, no 4, pp. 239–243, Jul. 2017. https://doi.org/10.1109/JEDS.2017.2706676

[15] Zhe Chen, Wei Hong, Jixin Chen, and Jianyi Zhou, "Design of High-Q Tunable SIW Resonator and Its Application to Low Phase Noise VCO" IEEE Microw. Wirel. Compon. Lett., vol. 23, no 1, pp. 43–45, Jan. 2013. https://doi.org/10.1109/LMWC.2012.2234088

[16] Y. Kobayashi and T. Senju, "Resonant modes in shielded uniaxial-anisotropic dielectric rod resonators," in IEEE Transactions on Microwave Theory and Techniques, vol. 41, no. 12, pp. 2198-2205, Dec 1993. https://doi.org/10.1109/22.260706

[17] K. Savin, Yu. Prokopenko and G. A. E. Vandenbosch, "Mode matching technique for tunable shielded cylindrical metal-dielectric resonator," 33d IEEE Int. Conf. "Electronics and Nanotechnology" (ELNANO-2013), Kyiv, Ukraine, 16–19 April 2013, pp. 118–122. https://doi.org/10.1109/ELNANO.2013.6552054

[18] K. Savin, I. Golubeva, Y. Prokopenko, "Calculation of frequency and power characteristics of the composite metal-dielectric resonator using the method of partial regions," Radioelectronics and Communications Systems, vol. 59, no.5, p. 229–236, May 2016. https://doi.org/10.3103/S0735272716050058

[19] G. N. Brooke and M. Z. Kharadly, "Field behaviour near anisotropic and multidielectric edges", IEEE Trans. Antennas Propagat., vol. AP-25, no. 4, pp. 571–575, July 1977. https://doi.org/10.1109/TAP.1977.1141646

[20] I. N. Bondarenko, Y. S. Vasiliev, A. S. Zhizhiriy and A. L. Ishenko, "Arrangement device for monitoring of parameters of microwave resonators," *2010 20th International Crimean Conference "Microwave & Telecommunication Technology"*, Sevastopol, 2010, pp. 969-970. https://doi.org/10.1109/CRMICO.2010.5632420

[21] Pratsiuk Borys, Prokopenko Yuriy, Poplavko Yuriy. Tunable filters based on metal-dielectric resonators // Proc. of 18th International Conference on Microwave, Radar and Wireless Communications MIKON-2010, June 14-16. – pp. 309-311.

[22] Yu. V. Prokopenko, "Controllability range of dielectric inhomogeneity located between the metal planes," Tekhnologiya i Konstruirovanie v Elektronnoi Apparature, no. 6, pp. 16-20, Nov. 2012 (in Russian).

[23] K. Savin, P. Sergienko, I. Golubeva, Y. Prokopenko, "Calculation of quality factor of tunable shielded cylindrical metal-dielectric resonator using mode matching technique," Proc. of 20th International Conference on Microwave, Radar and Wireless Communications MIKON-2014, Gdansk (Poland), June 16-18, pp. 414-416. https://doi.org/10.1109/MIKON.2014.6899952